Intermittency in the two-dimensional inverse cascade of energy: Experimental observations

Jérôme Paret and Patrick Tabeling
Laboratoire de Physique Statistique, Ecole Normale Supérieure, 24 rue Lhomond, 75231 Paris Cedex 05, France

(Received 17 March 1998; accepted 25 August 1998)

An extensive experimental study of the two-dimensional inverse energy cascade is presented. The experiments are performed in electromagnetically driven flows, using thin, stably-stratified layers. Complete instantaneous velocity fields are measured using particle imaging velocimetry techniques. Depending on the bottom-wall friction, two different regimes are observed: when the friction is low, the energy transferred from the forcing scale towards large scales accumulates in the lowest accessible mode, leading to a mean rotation of the flow and to an energy spectrum displaying a sharp peak at the minimum wave-number. This condensation is accompanied by the emergence of a very strong vortex around which the rotation is organized. At higher frictions, the inverse energy cascade conjectured by Kraichnan [Phys. Fluids **10**, 1417 (1967)] is observed and is found to be stationary, homogeneous and isotropic, with a Kolmogorov constant consistent with numerical estimates. This inverse cascade does not appear to be characterized by the presence of strong coherent vortices. The characteristic size of the latter is of the order of the injection scale. Their statistical properties tend to show that the cascade is rather driven by a clustering mechanism involving same sign vortices rather than a sequence of merging events producing larger and larger vortices. Intermittency effects are also investigated for the inverse cascade range. It is found that, within experimental errors, there is no intermittency in the inverse cascade range of two-dimensional turbulence and that the statistics of velocity increments, either longitudinal or transverse, are close to Gaussian. These results constitute the first experimental study of intermittency in two-dimensional turbulence as well as the first observation of normal scaling in a field of research which has been increasingly concerned with anomalous exponents. © *1998 American Institute of Physics.* [S1070-6631(98)01212-4]

I. INTRODUCTION

Two-dimensional turbulence is characterized by the conservation of the vorticity of each fluid parcel in the inviscid limit. These conservation laws imply the existence of two quadratic invariants: the energy and the enstrophy. These two constraints led Kraichnan to conjecture in 1967 the existence of two different inertial ranges for two-dimensional (2D) turbulence:[1] one with constant energy flux extending from the injection scale toward larger scales and one with constant enstrophy flux extending from the injection scale down to the viscous scale. The first one is known as the inverse energy cascade range and Kraichnan predicted an energy spectrum scaling as $k^{-5/3}$ for this range. The second one is called the direct enstrophy cascade range and was proposed to present a k^{-3} scaling for the energy spectrum, a scaling later modified with a logarithmic correction due to the nonlocality of interactions in this direct range.[2] Moreover, Kraichnan conjectured that in the absence of any dissipation mechanism removing energy from the system at large scales, the energy should condensate in the lowest accessible mode of the system, a process similar to Bose–Einstein condensation.

Since then, these predictions have been tested in several numerical simulations. The universality of the direct cascade range still appears to be questionable: typically, energy spectra steeper than k^{-3} were observed[3,4] although recent series of very high resolution simulations performed by Borue[5] show a scaling much closer to the expected k^{-3} law. This nonuniversality has been related to the presence of strong coherent vortices in the enstrophy cascade range although their exact influence is still unclear. The inverse cascade range, however, appears to be more robust: almost all numerical simulations performed on the subject[4,6–11] support the existence of the $k^{-5/3}$ scaling law. At late stages of the simulations by Smith and Yakhot[9,10] and in the simulations by Hossain *et al.*,[12] the condensation of energy was observed, together with the emergence of strong vortices.

On the experimental side, there do not exist many observations for forced two-dimensional turbulence. Experiments performed in soap films[13,14] displayed energy spectra consistent with the Kraichnan predictions for both inertial ranges but were not clear enough to be fully conclusive. In 1986, Sommeria observed both the inverse cascade and the condensation[15] although using measurement techniques which did not allow him to access the complete velocity fields. Recently,[16] using thin stratified layers of electromagnetically forced electrolytes, we observed an inverse energy cascade with a clear $k^{-5/3}$ scaling and measured a Kolmogorov constant consistent with numerical estimates. Since this scaling now seems to be well established, it is natural to ask

whether there exist intermittency corrections as for the three-dimensional cascade of energy.

Intermittency is perhaps the most studied problem in the field of turbulence. It is well known, both from experimental and numerical observations, that in three-dimensional turbulence the scaling exponents of the high-order statistics of velocity differences deviate from the values stemming from Kolmogorov 1941 theory.[17] Whether these deviations would survive in the limit of infinite Reynolds numbers is still an open question but all existing experiments and numerical simulations, at various Reynolds numbers, display anomalous exponents which seem to be universal. For two-dimensional turbulence, the issue is rather unclear. It is generally believed that the infinite number of inviscid integrals of motion and the presence of strong coherent structures make universality in 2D turbulence very unlikely. However, it should be noticed that the forced and decaying cases are much more different in 2D turbulence than they are in 3D turbulence. This means that, even if coherent structures play a dominant role in decaying 2D turbulence, as recognized by many authors,[18–21] they may be of secondary importance in the forced case. For the forced case, not much is known: some theoretical results have been proposed for the enstrophy cascade[22,23] but for the inverse cascade, the situation is puzzling. A numerical study by Babiano *et al.*[11] aimed at measuring the structure functions exponents suggests intermittency corrections, whereas the numerical simulations by Smith and Yakhot[9,10] show that the statistics of velocity differences in a developing inverse cascade are close to Gaussian, a fact which indicates the absence of sizable intermittency effects.

In this paper, we present an extensive experimental study of the inverse cascade of energy for two-dimensional turbulence. We observe experimentally the existence of both the inverse cascade and the condensate regime. In the condensate regime, we observe the steepening of the energy spectrum at large scales, and the emergence of a strong global rotation organized around a central vortex with high vorticity levels. For the inverse cascade regime, we investigate in detail intermittency effects. Studying both longitudinal and transverse statistics, we find that the inverse cascade is nonintermittent and that the statistics of velocity increments are close to Gaussian. These experimental results are fully consistent with the high resolution numerical simulations performed by Smith and Yakhot.[9,10] They constitute the first experimental study of intermittency for forced two-dimensional turbulence and the first observation of normal scaling in the field of fully developed turbulence.

The outline of the paper is as follows: in Sec. II we present the experimental set-up, outlining its advantages. We also discuss several aspects of data processing and analyze with some detail the statistical convergence of the moments and the determination of error bars. The main body of the paper is constituted by Sec. III in which we present and discuss the results for the stationary regimes for which the energy spectrum follows the Kraichnan–Kolmogorov scaling, $E(k)=C_K\varepsilon^{2/3}k^{-5/3}$. Both longitudinal and transverse statistics are considered. Moreover, we present results concerning the vortex properties of the flow. In Sec. IV, we present results on the condensation regime which appears when the cascade reaches the size of the flow domain. Finally, in Sec. V, we summarize our results and present conclusions.

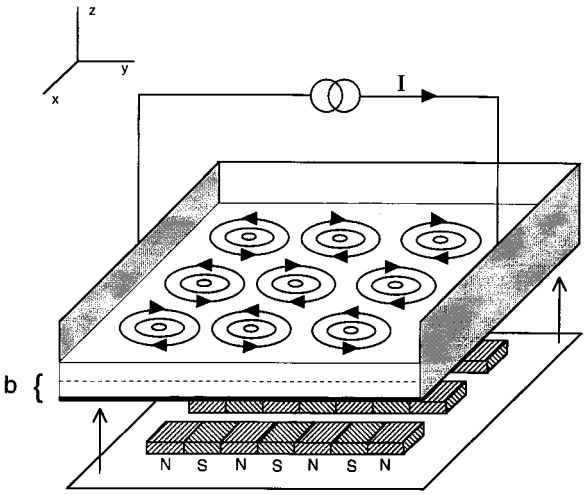

FIG. 1. The experimental set-up.

II. EXPERIMENTAL SET-UP

There are several methods for imposing the dynamics of a flow to be quasi two-dimensional. All of them use imposed external parameters such as aspect ratio, rotation, stratification or a magnetic field in the case of conducting fluids. We make use of two of these constraints to investigate two-dimensional turbulence in the laboratory: the aspect ratio and the stratification.

A. The experimental flows

The experimental device we use has been described in a number of previous papers (see Cardoso *et al.*[24] for a detailed description, although without the use of stratification). It is presented in a schematic way in Fig. 1. The flow is generated in a 15 cm×15 cm cell. The cell is filled by two layers of NaCl solution, placed in a stable configuration, i.e., the heavier underlying the lighter. Permanent magnets are located just below the bottom of the cell. Their magnetization axis is vertical and they produce a magnetic field, 0.3 T in maximum amplitude, which decays over a typical length of 3 mm. An electric current is driven through the cell from one side to the other. The interaction of this current with the magnetic field produces Laplace forces which drive the flow. Experiments carried out on simple flows have shown[25] that this device generates flows which are really two-dimensional. The main dissipation in this system is provided by the friction exerted by the bottom wall on the fluid. It can be parametrized by adding a linear term in the two-dimensional Navier–Stokes equations. This frictional term, if large enough, provides the infra-red energy sink preventing the condensation of energy in the lowest accessible mode. It can be varied by changing the total fluid depth but

the range of allowed depths is not wide since it is clear that a large fluid depth would ruin the two-dimensionality assumption.

The flow is visualized by tiny latex particles placed at the free surface. During the experiment, the flow is recorded on a video tape using a CCD camera placed above the cell. The images are digitized and stored on a computer. We then use standard particle imaging velocimetry (PIV) techniques to compute the velocity fields at any time. These fields are evaluated on 64×64 grids. From the velocity fields we can eventually compute any quantity we need for the analysis of the experiments: vorticity fields, stream function, energy spectra, structure functions (either longitudinal or transverse), probability density functions of velocity differences, ... The main advantage of our experimental device is that it allows us to study both the longitudinal and transverse parts of the velocity differences statistics, which is difficult to do in three-dimensional turbulence. Moreover, even if we do not use this fact in the present study which deals with stationary and homogeneous flows and spatial statistics, it allows us to analyze separately the spatial and temporal behaviors of the flows. Finally, just by changing the magnet arrangement or the driving electric current, we are able to investigate a wide class of flows. It will allow us to study the direct enstrophy cascade in the near future.

In the experiments we present here, the magnets are arranged in such a way that the flow is initially concentrated around a prescribed large wave-number. The injection scale l_i is about 1.5 cm, which is one tenth of the box size. We use total fluid depths of 5.5 mm for the stationary inverse cascade regime (Sec. III) and 7.5 mm for the condensation regime (Sec. IV). The imposed current, which, coupled to the magnetic field, defines the forcing, is a time series of impulses of constant amplitude and random sign. Each elementary impulse has a duration of 4 s, which is longer than the characteristic time of vertical transfers (the latter is shorter than 2 s).[25] The random-in-time forcing allows the imposition of an approximately zero net flow, which favors homogeneity. The current is switched on at $t=0$ and the flow is recorded for a typical time of 6 minutes: this corresponds to approximately 50 turn-over times of the largest eddies. Longer experiments are possible in order to enhance statistical convergence but for experiments longer than 10 minutes, the stratification progressively disappears because of diffusion between the two layers, and two-dimensionality can be lost in the process. We have thus turned back to ensemble averaging: the probability density functions we will present were obtained through averaging 10 identical experiments, each having a 5 minute duration. All the experiments have a typical injection Reynolds number (based on the root-mean-square velocity and the injection scale l_i) around 100.

B. Data analysis

First, let us define the quantities which will be the objects of our analysis. Most studies about turbulence are concerned with the statistical properties of velocity differences between two points in the fluid domain taken at the same time t, these objects being considered as random variables. We will thus be interested in the moments of the distributions of the following variables:

$$\delta\mathbf{v}(\mathbf{x},\mathbf{r},t)=\mathbf{v}(\mathbf{x}+\mathbf{r},t)-\mathbf{v}(\mathbf{x},t).$$

At this point, the averages that must be computed are ensemble averages, which are averages over several realizations of the same flow. However, if the flow is stationary, homogeneous and isotropic, which has been checked for our experiments,[16] we can drop the dependences on time t, position $\mathbf{x}$ and orientation of the separation vector $\mathbf{r}$. We are thus left with

$$\delta\mathbf{v}(\mathbf{x},\mathbf{r},t)=\delta\mathbf{v}(r),\quad r=|\mathbf{r}|.$$

$\delta\mathbf{v}(r)$ is a random vector variable which we finally split into its longitudinal $\delta v_{\parallel}$ and transverse $\delta v_{\perp}$ components defined by

$$\delta v_{\parallel}(r)=\delta\mathbf{v}(r)\cdot\mathbf{r}/r,\quad \delta v_{\perp}(r)=\delta\mathbf{v}(r)\cdot\mathbf{r}^{\perp}/r,\quad \mathbf{r}^{\perp}=\mathbf{e_z}\times\mathbf{r},$$

in which $\mathbf{e_z}$ is the out-of-plane unit vector. In the following, all the averages we compute are ''total'' averages, i.e., averages over realizations, time, position and orientation of the separation $\mathbf{r}$.

Before turning to the results of our experiments, let us discuss the crucial issues of statistical convergence and accuracy of measurements of high-order moments and their scaling exponents. We are concerned with the structure functions of the velocity fields which are defined by

$$S_n^{\parallel}(r)=\langle|\delta v_{\parallel}(r)|^n\rangle,\quad S_n^{\perp}(r)=\langle|\delta v_{\perp}(r)|^n\rangle.$$

It must be noticed here that we use *absolute values* in the definition. It does not change anything for even-order moments, but for odd-order moments, it eliminates cancellations between positive and negative contributions which lead to a different behavior when the absolute value is not taken. The odd-order moments taken without the absolute value will be discussed in Sec. III E. One easy way to compute the above structure functions consists in summing the n-th power of the absolute value of all the r-separated velocity increments we can form out of the velocity fields at hand and then dividing by the total number of pairs of points entering the sum. However, by doing so, we do not have any information on the accuracy of values obtained in such a manner: would these values be modified if we had 10, 1000 or one million times as many points? This is the convergence issue. It can be partially addressed by using the following definition for the structure functions:

$$S_n^{\parallel}(r)=\int_{-\infty}^{+\infty}|v|^n p_r^{\parallel}(v)dv,\quad S_n^{\perp}(r)=\int_{-\infty}^{+\infty}|v|^n p_r^{\perp}(v)dv,$$

where $p_r^{\parallel}(v)$ $(p_r^{\perp}(v))$ is the probability of measuring over a separation r a longitudinal (transverse) increment lying between v and $v+dv$. An approximation of these asymptotic probability density functions (PDF) is obtained when plotting the histogram of all the velocity increments that have been measured for a separation r. The curves $|v|^n p(v)$ then provide a way to check the statistical convergence of data. As the order n becomes larger these curves pick up the far tails of the PDF, which are not well resolved. Therefore, the

main contribution to the above integrals for large n comes from the noisy parts of the curve. Determining a reasonable value for the integral would thus involve some arbitrary filtering process which we will not do. We will limit ourselves to orders for which these curves are reasonably well defined and smoothly decreasing to zero for large increments.

At first look, structure functions exponents do not seem to exist at all. Even on a log–log plot, the curves $S_n^{\parallel}(r) = f(r)$ have a concave shape different from the straight line that would have been obtained in the case of a pure power-law. This can be understood since the curve must go smoothly from a $S_n^{\parallel}(r) \propto r^n$ regime at small scales to a $S_n^{\parallel}(r) \propto r^0$ at scales larger than the integral scale L. Since our inertial range is rather modest (less than one decade), it is not surprising that we do not observe a power-law. This transition is not smooth on the spectra because of the localization of the forcing in wave-number space, and this is why a power-law scaling can, however, be observed for the spectra. Yet, we have found that using the so-called extended-self-similarity (ESS) which consists in plotting $S_n^{\parallel}(r)$ as a function of $S_3^{\parallel}(r)$, one can accurately measure exponents. The exponents we will present in the next section were not determined by a power-law fit but rather by computing the logarithmic slope of the curve $S_n^{\parallel}(r) = f(S_3^{\parallel}(r))$ and looking for a plateau on the graph on which this slope is plotted as a function of the separation r. This allows to determine an error bar for the measured exponents by considering the maximum deviation from the mean value of the slope inside such a scaling range.

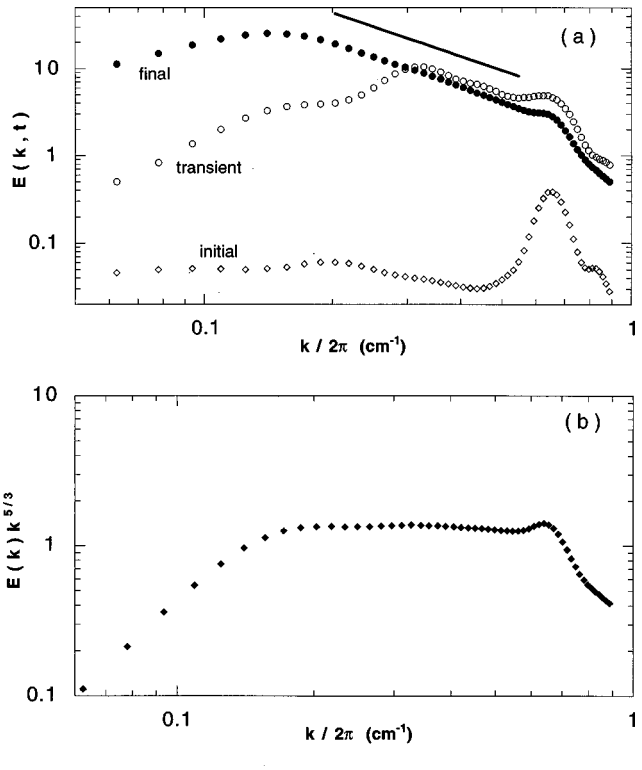

FIG. 2. Energy spectra. (a) Temporal evolution; (b) compensated energy spectrum for the stationary regime.

III. THE INVERSE CASCADE REGIME

We now turn to the results we have obtained for the inverse cascade regime. We begin with the results concerning the spectral properties of this regime (Sec. III A). We then present the properties of the vorticity fields and discuss the role of coherent structures in the inverse cascade range. Finally we present the observed statistics of the velocity increments, both longitudinal and transverse and show the definite existence of a ''flux state.''

A. Spectral properties

Our experiments show that, after a short transient of about 4 turn-over times, a stationary state is achieved. It can be maintained for rather long times, the only limitation we found being due to the loss of stratification which is crucial to two-dimensionality. Moreover, this stationary regime is statistically homogeneous. Its spectral properties are displayed in Fig. 2. The temporal evolution of the energy spectrum is shown in Fig. 2(a). The initial spectrum ($\diamond$) is computed just after the current has been switched on. It shows that the injection wave-number is well defined and that the forcing we apply really takes place at small scales. The second spectrum ($\circ$), computed in the transient regime, displays the progressive build-up of the $-5/3$ scaling, as was conjectured by Kraichnan[1] and numerically observed by Smith and Yakhot.[9,10] Finally, the last spectrum ($\bullet$) is the average spectrum for the stationary regime. It displays a $k^{-5/3}$ behavior over a range slightly narrower than one decade (the black line is a reference $-5/3$ scaling). We display the compensated spectrum $E(k)k^{5/3}$ in Fig. 2(b). A clear plateau can be seen in the same range of scales for which the scaling law is observed in 2(a). This shows that, even if the scaling range is not wide, the spectral behavior we observe is in remarkable agreement with the Kraichnan prediction:

$$E(k) = C_K \varepsilon^{2/3} k^{-5/3}.$$

Using three different methods,[16] we measured ε and determined the Kolmogorov constant to be about 6.5, a value consistent with numerical estimates[4,9,10] and tending to show that this constant is probably universal. A fourth method, involving the third-order longitudinal structure function, taken *without absolute values*, will be discussed in the following (Sec. III E).

In order to show that this scaling corresponds to inverse transfers (from small to large scales), we have computed the spectral energy flux $\Pi(k)$ which is the flux of energy transferred from wave-numbers smaller than k to wave-numbers larger than k. A detailed expression for $\Pi(k)$ can be found, for example, in the paper by Kraichnan.[1] The results are displayed in Fig. 3. It can be seen that $\Pi(k)$ is negative for wave-numbers smaller than the injection wave-number k_i, thus showing that the energy transfers are toward large scales for the $k^{-5/3}$ scaling range. Due to the moderate width of the scaling range and to the low spectral resolution, we do not observe a plateau with $\Pi(k) = -\varepsilon$. However, the latter relation holds at the inflection point in the middle of the scaling range. It seems likely that this inflection point would develop into a plateau if we had a larger scaling range.

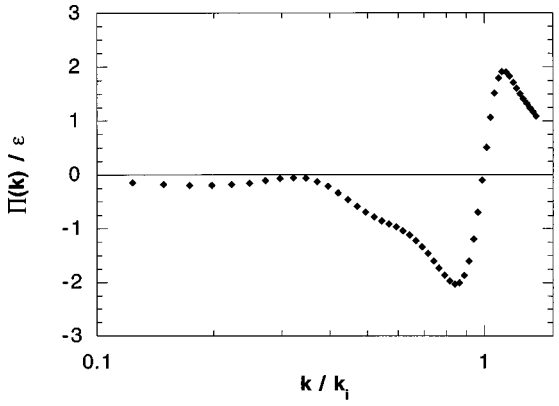

FIG. 3. Spectral energy flux $\Pi(k)$ as a function of wave-number k. $\Pi(k)$ is rescaled by ε and k by the injection wave-number k_i.

The isotropy of the flow is not straightforward: since the experiments are performed in a square box using an anisotropic forcing, one may expect that these deviations from isotropy would propagate within the inertial range. However, it is not so: we observed that the anisotropy due to the forcing relaxed rapidly, yielding an almost isotropic inertial range. It can be seen in Fig. 4 in which we display the two-dimensional energy spectrum $E(k_x,k_y)$ for the stationary regime. The forcing wave-number is signaled by the four closed contours on each side of the plot and makes the corresponding scales anisotropic but the inertial range scales (toward the center of the plot) are not affected by this anisotropy. However, because of the box geometry, a slight anisotropy is recovered at large scales (center of the plot). These observations show that the cascade mechanism involves an efficient ''isotropization'' of the flow.

B. Vortex properties

Let us present the physical space characteristics of this inverse energy cascade and more precisely its consequences

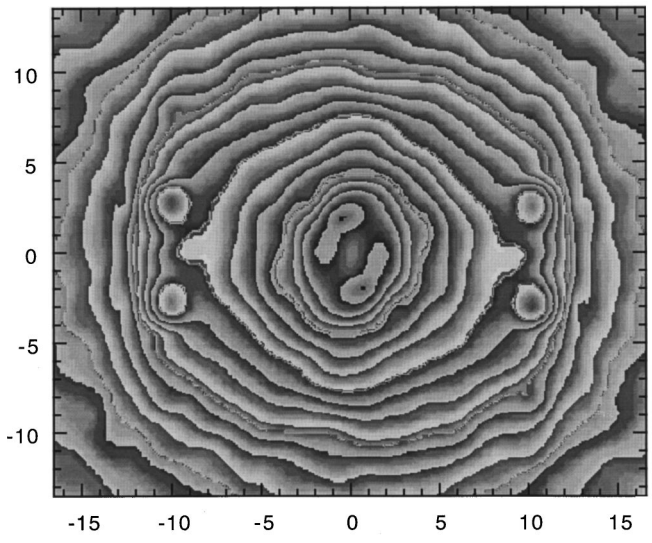

FIG. 4. Two-dimensional energy spectrum $E(k_x,k_y)$. Wave-numbers are rescaled by the smallest wave-number $k_{\min}=2\pi/L$ where L is the size of the box.

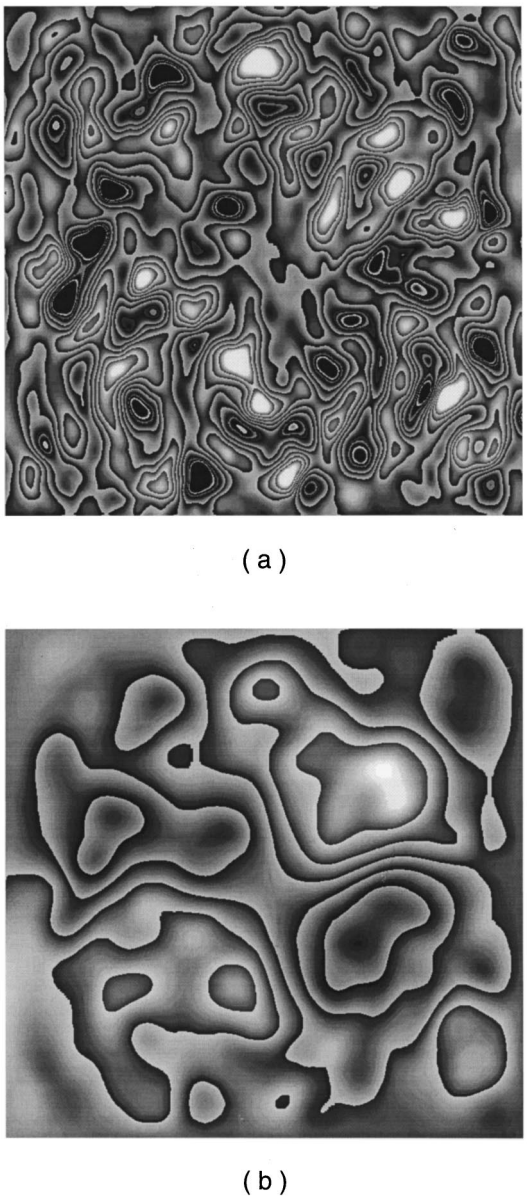

FIG. 5. Typical vorticity field (a) and stream function (b) in the inverse cascade regime.

in term of coherent structures. A typical vorticity field is displayed in Fig. 5(a) together with the corresponding stream function field [Fig. 5(b)]. It can be seen that there exist structures of various sizes but that axisymmetric structures that can be identified with vortices are rather small in size. It can be understood from the shape of the energy spectrum. This shape implies that the enstrophy spectrum $Z(k)$ has a maximum value when k is equal to the injection wave-number. Actually, we have $Z(k)=k^2E(k)$ and since $E(k)$ scales as $k^{-5/3}$ for $k\leqslant K_i$ and as k^{-n} with $n\geqslant 3$ for $k\geqslant K_i$, the above conclusion is straightforward. This shape of the enstrophy spectrum implies that, if there are vortices in the flow, they should have a characteristic size of the order of the injection scale. This is confirmed by the distribution of vortex sizes displayed in Fig. 6. Vortex sizes are determined by thresholding the vorticity fields at ± 1.5 times the root-mean-square value of the vorticity and measuring the size of the regions

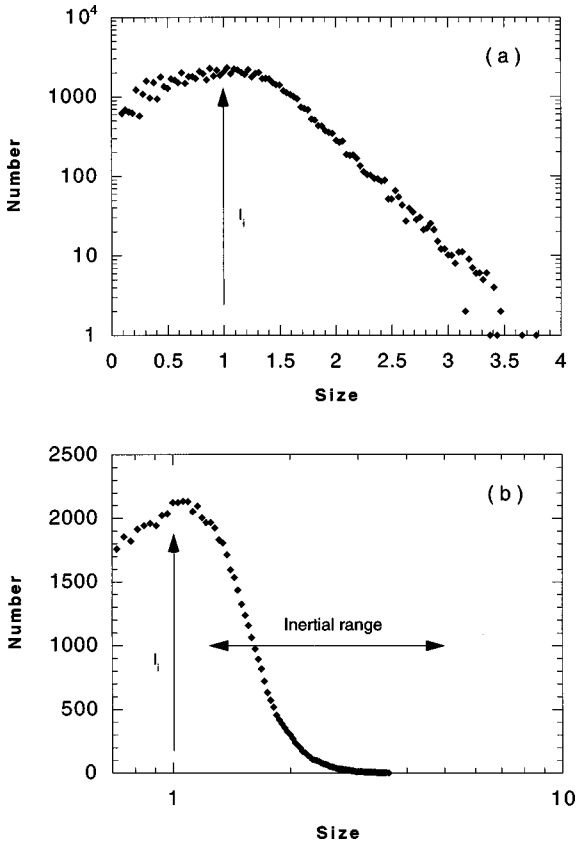

FIG. 6. Distribution of vortex sizes displayed using lin–log scales (a) and log–lin scales (b). Sizes are normalized by the injection scale l_i. The extension of the inertial range is displayed on part (b).

for which the absolute value of the vorticity is above the threshold. The use of lin–log scales [part (a) of the figure] makes it clear that this distribution is a decreasing exponential function of the vortex radius r for sizes corresponding to the inverse cascade. Plotting this distribution using log–lin scales and representing the extension of the scaling range [part (b) of the figure] shows that there are essentially no coherent structures of size corresponding to the inertial range scales. This point had already been recognized by Maltrud and Vallis.[4] This is certainly the most striking difference between decaying and forced two-dimensional turbulence. These characteristics of the vorticity field may also be a hint of the physical mechanism underlying the inverse cascade. It is sometimes considered that the inverse cascade is made of a sequence of merging events between same sign vortices as is the case in decaying turbulence. However, should it be so, the distribution of vortex sizes should be broad and probably not an exponentially decreasing function. Moreover, we have observed that such merging events were rare. The inverse cascade should rather be an aggregation process, that is the formation of large clusters of same sign vorticity. This picture is favored when looking at the stream function [Fig. 5(b)]: it can be seen that closed streamlines define large scale regions containing several same sign vortices [for example, the five ''white'' vortices in the upper-right corner of Fig. 5(a) are all enclosed within closed streamlines]. This aggregation progress can also be seen during the transient regime

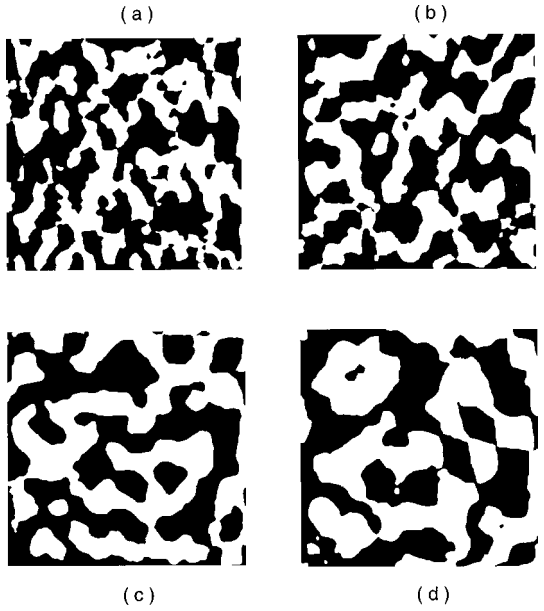

FIG. 7. Vorticity field in the transient regime for $t=2$ s (a), 6 s (b), 10 s (c) and 22 s (d) (white: $\omega \geqslant 0$; black: $\omega \leqslant 0$).

of our experiments. Figure 7 displays, at 4 different times in the transient regime, the regions of positive (white) and negative (black) vorticity: it can be seen that, as the cascade builds up, the vorticity tends to segregate and form larger and larger patches of the same sign. Finally, in order to quantitatively compare the characteristics of our vorticity fields with those of previous numerical simulations,[4,8] we have measured the kurtosis of the vorticity field K_ω and that of the stream function K_ψ defined by

$$K_\omega = \frac{\langle \omega^4 \rangle}{\langle \omega^2 \rangle^2}, \quad K_\psi = \frac{\langle \psi^4 \rangle}{\langle \psi^2 \rangle^2}.$$

We find that they are both constant in time during the stationary regime and that $K_\omega \approx 5$, $K_\psi \approx 3$. The value of K_ω is slightly lower than that found by Herring and McWilliams[8] but both K_ω and K_ψ are in remarkable agreement with the values given by Maltrud and Vallis.[4]

C. Longitudinal statistics

We now turn to the statistics of velocity increments. Let us begin with longitudinal ones $\delta v_\parallel(r)$. Great emphasis has always been put on them because they are the only measurable quantities for most experiments on three-dimensional turbulence, although some techniques are now being developed for measuring transverse increments. Intermittency can be characterized using several methods: it can be signaled by a nonlinear dependence of the scaling exponents ζ_n on the order n, by a scale dependence of the normalized moments of the PDF or by a dependence of the PDF shapes on the separation r. All three methods are used in the following, and we begin by the determination of scaling exponents. The longitudinal structure functions $S_n^\parallel(r)$ are displayed in Fig. 8 for $n=4$, 6, 8 and 10. They are plotted as a function of the nondimensional scale $l=r/l_i$ [Fig. 8(a)] and as a function of $S_3^\parallel(r)$ [Fig. 8(b)]. It is clear that if we try to define a scaling

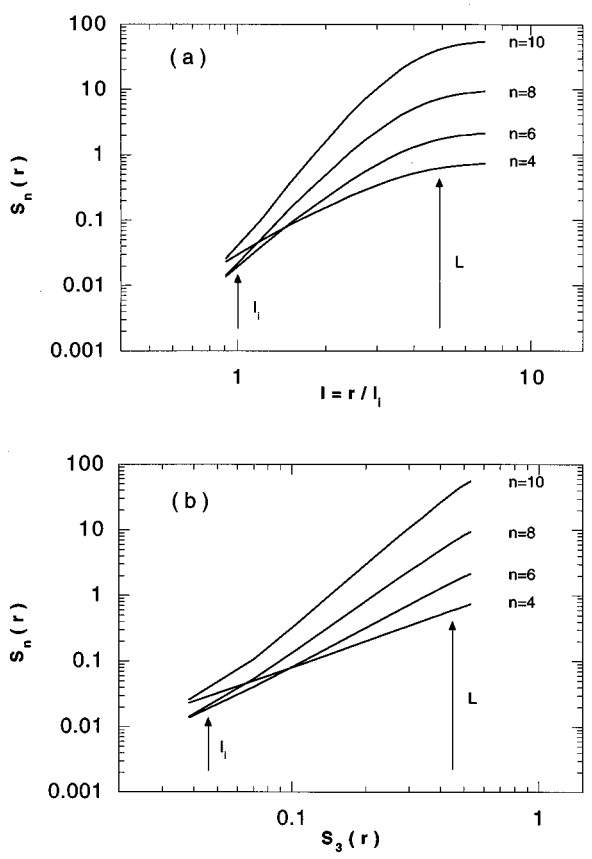

FIG. 8. Longitudinal velocity structure functions $S_n^{\parallel}(r)$ as a function of (a) the nondimensional scale $l=r/l_i$ and (b) $S_3^{\parallel}(r)$ for $n=4$, 6, 8 and 10. The injection scale l_i and the integral scale L are indicated.

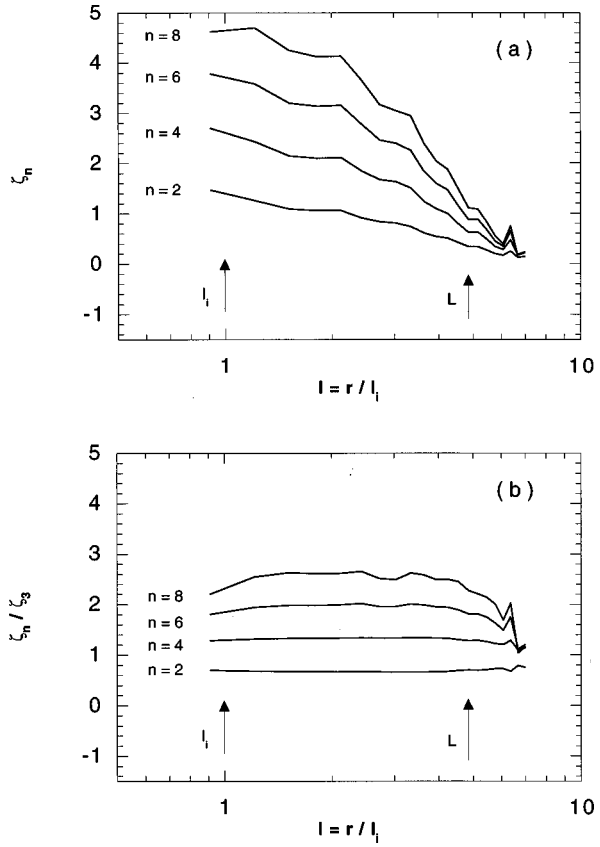

FIG. 9. (a) Local absolute scaling exponents ζ_n and (b) local relative scaling exponents $\widetilde{\zeta_n}=\zeta_n/\zeta_3$ as a function of the nondimensional scale $l=r/l_i$ for orders $n=2$, 4, 6 and 8 (log–lin scale). The scales l_i and L are indicated.

range on the curves $S_n^{\parallel}(r)=f(r)$, its extension will be very small. However, using the ESS representation [Fig. 8(b)], the scaling range is rather well defined and its extension is the same as the extension of the $k^{-5/3}$ scaling observed on the energy spectrum (Fig. 2). It is even clearer if we plot the local exponents, i.e., the logarithmic slopes of the curves displayed in Fig. 8. These local exponents are displayed in Fig. 9. We have limited ourselves to orders $n=2$, 4, 6 and 8 for the sake of clarity. Absolute exponents ζ_n and relative exponents $\widetilde{\zeta_n}=\zeta_n/\zeta_3$ are plotted as a function of the nondimensional scale l on parts (a) and (b) of the figure, respectively. Obviously, absolute exponents vary continuously with scale whereas relative exponents are approximately constant over a range of scales identical to the range of wave-numbers over which the Kraichnan–Kolmogorov spectrum is observed. The relative exponents we have determined are given in Table I and displayed in Fig. 10. They correspond to the mean values of the local relative exponents inside the scaling range. The error bars were determined from the maximum deviation from these mean values. In order to make a comparison, we have plotted Kolmogorov scaling $\zeta_n=n/3$ (full line) and typical values for three-dimensional turbulence as published by Belin *et al.*[26] (dashed line). This figure calls for two important remarks. First, it can be seen that the scaling exponents for two-dimensional and three-dimensional energy cascades are definitely different: 3D exponents are well outside the error bars we have determined for our experiments. Secondly, the exponents we have measured are very close to the Kolmogorov scaling: even for orders 10, 11 and 12 for which we are at the limit of statistical convergence, the law $\zeta_n=n/3$ still lies within error bars (note the rapid growth of error for orders higher than 8).

We are now showing that the statistics of longitudinal velocity differences not only follow normal scaling but are also quasi-normal, i.e., their normalized even-order moments are very close to the Gaussian values and do not vary with scale. The normalized even-order moments, defined by

$$H_{2n}^{\parallel}(r)=S_{2n}^{\parallel}(r)/(S_2^{\parallel}(r))^n,$$

are displayed in Fig. 11. They are plotted as a function of the nondimensional scale $l=r/l_i$. The Gaussian values ($H_4=3$, $H_6=15$, $H_8=105$, $H_{10}=945$ and $H_{12}=10395$) are plotted as full straight lines: they cannot be distinguished from the experimental data for scales larger than the injection

TABLE I. Relative scaling exponents $\widetilde{\zeta_n}=\zeta_n/\zeta_3\pm\sigma$ for the longitudinal structure functions.

n	1	2	3	4	5	6	7	8	9	10	11	12
$\widetilde{\zeta_n}$	0.33	0.66	1.00	1.33	1.65	1.98	2.30	2.59	2.87	3.13	3.38	3.60
σ	0.02	0.02	–	0.02	0.03	0.04	0.06	0.10	0.15	0.21	0.30	0.40

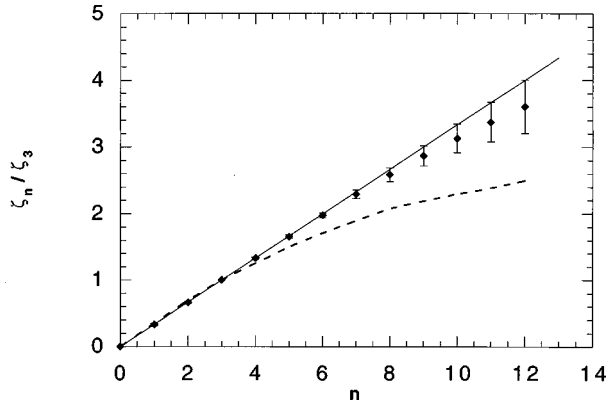

FIG. 10. Evolution of $\widetilde{\zeta_n}$ with n for $n \leqslant 12$. The full line corresponds to Kolmogorov scaling and the dashed line to the values for 3D turbulence (Ref. 26).

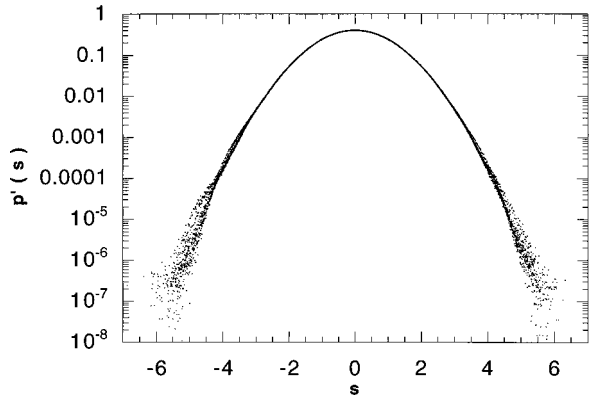

FIG. 12. Rescaled PDF of longitudinal velocity increments for 7 different separations in the inertial range. $s = \delta v / \langle \delta v^2 \rangle^{1/2}$.

scale l_i. Finally, Fig. 12 displays the probability density functions of longitudinal increments for 7 different separations in the inertial range. The PDF were rescaled by the following transformation:

$$\delta v \rightarrow \delta v' = \delta v / \langle \delta v^2 \rangle^{1/2},$$

$$p(v) \rightarrow p'(v') = \langle \delta v^2 \rangle^{1/2} p(v').$$

This transformation rescales all PDF to a unit variance so that their shapes can be compared. It can be seen that the shape does not vary with scale, thus showing the absence of any intermittency.

D. Transverse statistics

Let us now turn to the statistics of transverse increments. Since they should be more sensitive to vorticity and thus to coherent structures, one might expect them to be ''more intermittent'' than the longitudinal ones. The only known exact result about transverse statistics stems from isotropy and concerns the second-order structure functions. In two dimensions, it reads as

$$S_2^{\perp}(r) = (1 + r d/dr) S_2^{\parallel}(r).$$

As noticed by Babiano *et al.*,[27] this relation does not characterize isotropy but is only an implication of it. Figure 13 displays the three quantities $S_2^{\parallel}(r)$, $S_2^{\perp}(r)$ and $(1 + r d/dr) S_2^{\parallel}(r)$ for our experiments. The above relation appears to be rather well satisfied although not in a perfect way. However, the important point is that the transverse structure function displays a bump within the range of scales for which we had measured exponents for longitudinal structure functions. This bump is due to the above relation together with the fact that, at scales larger than the integral scale, we must have[27] $S_2^{\parallel}(r) \sim S_2^{\perp}(r) \sim 2E$ where $E = \langle \mathbf{v}^2 \rangle / 2$ is the energy of the flow. Although there is no relation such as the one above for higher orders, this bump is also present for all other transverse structure functions, even becoming sharper and sharper as the order increases. The range of scales for which exponents could be measured was not large for longitudinal structure functions, it is almost reduced to zero for transverse ones. We will not attempt to determine exponents from 4 or 5 points covering less than one octave of scales. A much larger inertial range is needed in order to accurately determine transverse exponents. However, we can still study intermittency using the normalized even-order moments and the PDF shapes. Results are displayed in Figs. 14 and 15, respectively. Here again, no intermittency can be seen.

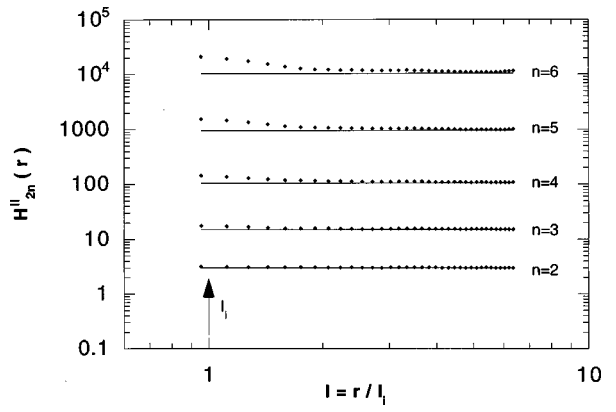

FIG. 11. Normalized longitudinal even-order moments $H_{2n}^{\parallel}(r)$ as a function of the nondimensional scale $l = r/l_i$ for $n = 2$, 3, 4, 5 and 6. Flat lines are the Gaussian values.

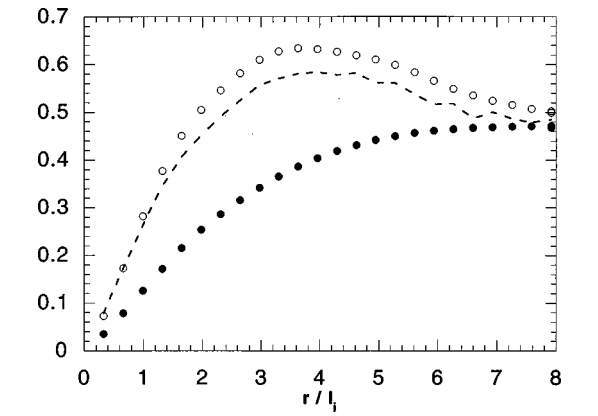

FIG. 13. $S_2^{\parallel}(r)$ (●), $S_2^{\perp}(r)$ (○) and $(1 + r d/dr) S_2^{\parallel}(r)$ (dashed line) vs the nondimensional scale $l = r/l_i$

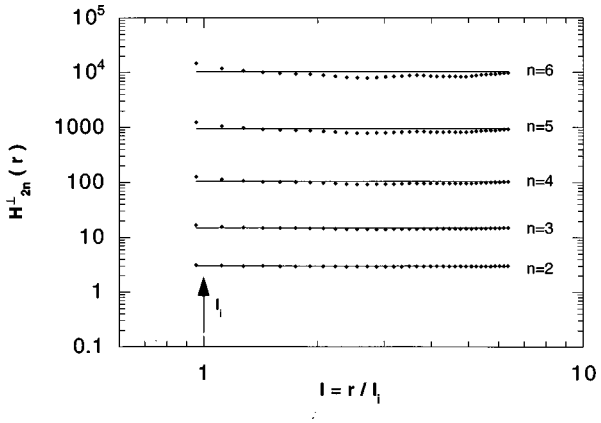

FIG. 14. Normalized transverse even-order moments $H^{\perp}_{2n}(r)$ as a function of the nondimensional scale $l=r/l_i$ for $n=2$, 3, 4, 5 and 6. Flat lines are the Gaussian values.

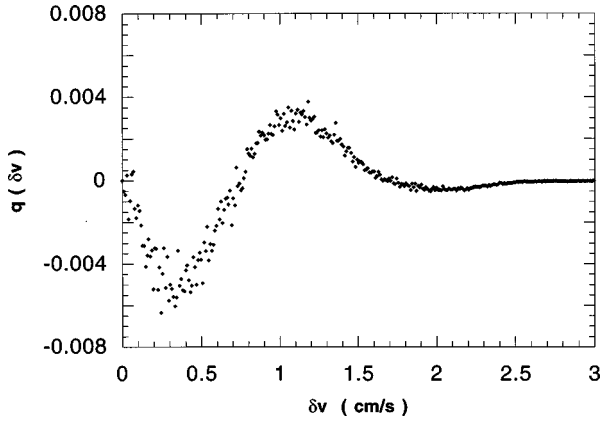

FIG. 16. Difference $q^{\parallel}_r(v)$ between the positive and negative contribution to a PDF of longitudinal increments for an inertial range separation r with $r/l_i=3.2$.

E. Asymmetry of longitudinal probability density functions

At this point, one may be a little puzzled: if the velocity increments statistics are Gaussian, is there any cascade at all? In three-dimensional turbulence, it is known that the PDF of longitudinal velocity increments are asymmetric and that this asymmetry is linked to the energy transfer rate through the third-order longitudinal structure function and the Kolmogorov ''$-4/5$'' law. If the PDF were Gaussian (thus symmetric), there would be no energy transfer and thus no cascade. Following closely the demonstration given by Frisch,[28] one can derive the following relation for the two-dimensional inverse energy cascade:

$$\langle (\delta v_{\parallel}(r))^3 \rangle = \frac{3}{2}\varepsilon r, \quad l_i \ll r \ll L,$$

in which the energy transfer rate ε is taken to be positive. It is perhaps less rigorous than its 3D counterpart since in the demonstration one must *assume* the relation

$$\Pi(K) = -\varepsilon, \quad \forall K \ll K_i,$$

but if we admit the existence of an inverse cascade, the above relation should hold. Such a relation could provide a fourth method to determine ε from the experimental data along with the three other we used.[16] We have actually found that this method cannot be used in practice. It can be understood in the following way: taking the above relation for the third-order longitudinal structure function along with the Fourier transform of the Kraichnan–Kolmogorov spectrum $E(k)=C_K\varepsilon^{2/3}k^{-5/3}$ with $C_k \sim 6.5$, one can get the following estimate for the skewness $S=S^{\parallel}_3(r)/S^{\parallel}_2(r)^{3/2}$ of velocity differences in the inertial range:

$$S \sim 0.05.$$

This value is too small to allow the detection of an asymmetry directly on the PDF. The fact that the value of the skewness is much smaller than in three-dimensional turbulence is linked to the Kolmogorov constant C_K, which is much higher in two than in three dimensions. This point had already lead Aref and Siggia to conjecture that intermittency would be weak and the statistics close to Gaussian in the inverse cascade.[6] In order to show that, even if we are not able to accurately measure the above third-order longitudinal structure function, our experimental data are consistent with the presence of energy transfers as shown in Fig. 3, we display in Fig. 16 the following quantity:

$$q^{\parallel}_r(v) = p^{\parallel}_r(v) - p^{\parallel}_r(-v), \quad v \geqslant 0$$

for a separation r lying in the inertial range ($r/l_i=3.2$). It can be seen that, even if the curve is rather noisy, the underlying shape is well defined, thus proving that the PDF in the inverse cascade range are definitely not symmetric. Note the positive and negative lobes which almost cancel each other when computing $\langle (\delta v_{\parallel}(r))^3 \rangle$.

All the above results show that what we have observed is the inverse energy cascade as described by Kraichnan. Moreover, we also obtain that the cascade is nonintermittent, with almost Gaussian statistics.

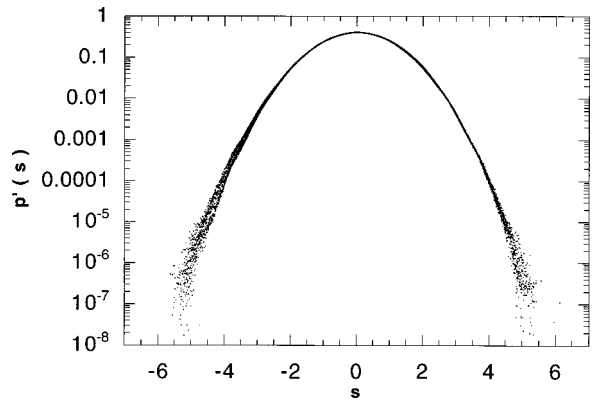

FIG. 15. Rescaled PDF of transverse velocity increments for 7 different separations in the inertial range. $s=\delta v/\langle \delta v^2 \rangle^{1/2}$.

IV. THE CONDENSATE REGIME

We now turn to the new regime which appears when the large scale energy sink is not strong enough to prevent the ''front'' of the cascade from reaching the size of the box. The existence and the main properties of such a regime had

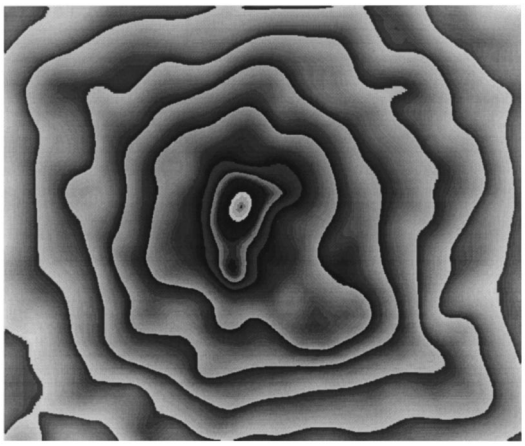

FIG. 17. Stream function in the condensation regime.

already been conjectured by Kraichnan.[1] He compared it to the Bose–Einstein condensation, a terminology which remains. The condensation has been observed experimentally by Sommeria[15] and numerically by Hossain *et al.*[12] and more recently by Smith and Yakhot.[9,10] The basic mechanism of this regime is the accumulation of energy in the lowest accessible mode. The structure of the flow can then depend on boundary conditions. In our experiments, which are carried out in a square box, we find, as did Sommeria, that the flow is dominated by a strong mean rotation even if the forcing injects an approximately zero net circulation. With periodic boundary conditions, Smith and Yakhot observed the formation of a vorticity dipole with increasingly strong vorticity at the core of the vortices. Let us first qualitatively show how different the two regimes are: Fig. 17 displays the stream function for the condensate regime. Whereas a large range of sizes can be seen in the inverse cascade regime [Fig. 5(b)], only does the global rotation remain in the condensed state. More quantitatively, we display the energy spectrum for the condensate regime in Fig. 18: this spectrum displays a sharp bump at large scales and no scaling range can be observed. This behavior at large scales is consistent with the picture of the mechanism above and with observations by Sommeria.

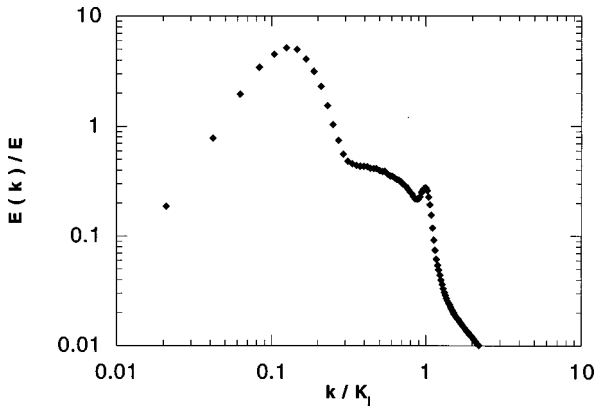

FIG. 18. Energy spectrum in the condensation regime. Wave-numbers are rescaled by the injection scale and modal energies are rescaled by the total energy.

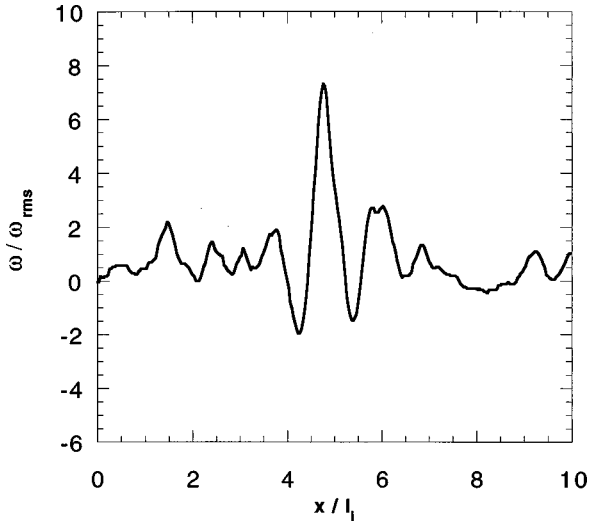

FIG. 19. Vorticity profile along a cross-section of a vorticity field in the condensation regime. Vorticities ω are rescaled by the root-mean-square value ω_{rms}; positions x are rescaled by the injection scale l_i.

Moreover, this bump has a scaling consistent with a k^{-3} law although it is not developed enough in order to draw a definite conclusion.

Finally, we have observed the interesting phenomenon of vorticity intensification identified numerically by Smith and Yakhot. We have found that the instantaneous vorticity fields were still perturbed by small scales fluctuations due to the low Reynolds number achieved but that they displayed a single central vortex with a rather deep core around which the mean global rotation was organized. A vorticity profile along a line passing through this vortex is displayed in Fig. 19. It can be seen that the central vortex is much stronger than the fluctuations on the sides. The further evolution of this vortex cannot be decided from our experiments. Would it become stronger and stronger as time goes by, as observed by Smith and Yakhot, then saturate and stay stable or would it become unstable and break into small very strong vortices? Very high Reynolds numbers are needed to decide on this point. However, the early observations by Sommeria tended to show that the mean global rotation was very robust.

V. CONCLUSION

In this paper, we have presented a comprehensive experimental study of the inverse energy cascade of two-dimensional turbulence. By varying the dissipation at large scales, we have found that two very different regimes can exist as stationary states. When the integral scale of the flow becomes comparable to the size of the fluid domain, the inverse cascade experiences a condensation process. This behavior, early conjectured by Kraichnan[1] had already been observed experimentally by Sommeria[15] but we provided here the first experimental observation of the vortex intensification process numerically observed by Smith and Yakhot.[9,10]

When the integral scale was smaller than the box size, we observed the usual inverse energy cascade with Kraichnan–Kolmogorov scaling. The main observation of

our study is that this inverse cascade appears to be *nonintermittent*. The statistics of this inverse cascade are characterized by four main features.

(1) The role of coherent structures in the inverse cascade range is an open issue. The cascade is nonetheless driven by an aggregation process of these structures, rather than by merging events.
(2) Structure functions exponents are found to be equal, within experimental accuracy, to their Kolmogorov values $\zeta_n = n/3$.
(3) No significant difference is found between longitudinal and transverse statistics.
(4) Statistics of velocity increments are very close to Gaussian.

These observations make the two-dimensional inverse energy cascade look considerably different from its three-dimensional counterpart. Although higher Reynolds number and wider inertial ranges would be necessary to draw definitive conclusions, we hope that our results may serve as a basis for a theoretical treatment of the inverse cascade. The features we observed are appealing and an interesting issue is whether they are accessible to a theoretical explanation.

ACKNOWLEDGMENTS

This work was supported by Center National de la Recherche Scientifique, Ecole Normale Supérieure, Universités Paris 6 and Paris 7. We would like to thank A. Babiano, G.L. Eyink, G. Falkovich, S. Fauve, U. Frisch, V. Lebedev, V. L'vov, L.M. Smith, and V. Yakhot for interesting discussions concerning issues related to the inverse cascade. J.P. acknowledges B. Andreotti for fruitful discussions about errors determination and accuracy of the statistical analysis of data.

[1] R. H. Kraichnan, ''Inertial ranges in two-dimensional turbulence,'' Phys. Fluids **10**, 1417 (1967).
[2] R. H. Kraichnan, ''Inertial-range transfers in two- and three-dimensional turbulence,'' J. Fluid Mech. **47**, 525 (1971).
[3] B. Legras, P. Santangelo, and R. Benzi, ''High resolution numerical experiments for forced two-dimensional turbulence,'' Europhys. Lett. **5**, 37 (1988).
[4] M. E. Maltrud and G. K. Vallis, ''Energy spectra and coherent structures in forced two-dimensional and beta-plane turbulence,'' J. Fluid Mech. **228**, 321 (1991).
[5] V. Borue, ''Spectral exponents of enstrophy cascade in stationary two-dimensional homogeneous turbulence,'' Phys. Rev. Lett. **71**, 3967 (1993).
[6] E. D. Siggia and H. Aref, ''Point-vortex simulation of the inverse energy cascade in two-dimensional turbulence,'' Phys. Fluids **24**, 171 (1981).
[7] U. Frisch and P. L. Sulem, ''Numerical simulation of the inverse cascade in two-dimensional turbulence,'' Phys. Fluids **27**, 1921 (1984).
[8] J. R. Herring and J. C. McWilliams, ''Comparison of direct numerical simulation of two-dimensional turbulence with two-point closure: the effects of intermittency,'' J. Fluid Mech. **153**, 229 (1985).
[9] L. M. Smith and V. Yakhot, ''Bose condensation and small-scale structure generation in a random force driven 2D turbulence,'' Phys. Rev. Lett. **71**, 352 (1993).
[10] L. M. Smith and V. Yakhot, ''Finite-size effects in forced two-dimensional turbulence,'' J. Fluid Mech. **274**, 115 (1994).
[11] A. Babiano, B. Dubrulle, and P. Frick, ''Scaling properties of numerical two-dimensional turbulence,'' Phys. Rev. E **52**, 3719 (1995).
[12] M. Hossain, W. H. Matthaeus, and D. Montgomery, ''Long-time state of inverse cascades in the presence of a maximum length scale,'' J. Plasma Phys. **30**, 479 (1983).
[13] M. Gharib and P. Derango, ''A liquid film (soap film) tunnel to study two-dimensional laminar and turbulent shear flows,'' Physica D **37**, 406 (1989).
[14] H. Kellay, X. L. Wu, and W. I. Goldburg, ''Experiments with turbulent soap films,'' Phys. Rev. Lett. **74**, 3975 (1995).
[15] J. Sommeria, ''Experimental study of the two-dimensional inverse energy cascade in a square box,'' J. Fluid Mech. **170**, 139 (1986).
[16] J. Paret and P. Tabeling, ''Experimental observation of the two-dimensional inverse energy cascade,'' Phys. Rev. Lett. **79**, 4162 (1997).
[17] A. N. Kolmogorov, ''The local structure of turbulence in incompressible viscous fluid for very large Reynolds number,'' Dokl. Akad. Nauk. SSSR **30**, 9 (1941) [reprinted in Proc. R. Soc. London Ser. A **434**, 9 (1991)].
[18] J. C. McWilliams, ''The emergence of isolated coherent vortices in turbulent flows,'' J. Fluid Mech. **146**, 21 (1984).
[19] R. Benzi, S. Patarnello, and P. Santangelo, ''Self-similar coherent structures in two-dimensional decaying turbulence,'' J. Phys. A **21**, 1221 (1987).
[20] J. C. McWilliams, ''The vortices of two-dimensional turbulence,'' J. Fluid Mech. **219**, 361 (1990).
[21] G. F. Carnevale, J. C. McWilliams, Y. Pomeau, J. B. Weiss, and W. R. Young, ''Evolution of vortex statistics in two-dimensional turbulence,'' Phys. Rev. Lett. **66**, 2735 (1991).
[22] G. Falkovich and V. Lebedev, ''Universal direct cascade in two-dimensional turbulence,'' Phys. Rev. E **50**, 3883 (1994).
[23] G. L. Eyink, ''Exact results on stationary turbulence in 2D: consequences of vorticity conservation,'' Physica D **91**, 97 (1996).
[24] O. Cardoso, D. Marteau, and P. Tabeling, ''Quantitative experimental study of the free decay of quasi-two-dimensional turbulence,'' Phys. Rev. E **49**, 454 (1994).
[25] J. Paret, D. Marteau, O. Paireau, and P. Tabeling, ''Are flows electromagnetically forced in thin stratified layers two-dimensional?,'' Phys. Fluids **9**, 3102 (1997).
[26] F. Belin, P. Tabeling, and H. Willaime, ''Exponents of the structure functions in a low temperature helium experiment,'' Physica D **93**, 52 (1996).
[27] A. Babiano, C. Basdevant, and R. Sadourny, ''Structure functions and dispersion laws in two-dimensional turbulence,'' J. Atmos. Sci. **42**, 941 (1985).
[28] U. Frisch, *Turbulence: The Legacy of A. N. Kolmogorov* (Cambridge University Press, Cambridge, 1995).